

Ruthenium Thrifiting – Computation Insights in NH₃ Decomposition onto Ru Single Atom Catalyst CeO₂

Nomcebo P. Motsa^{a,*}, Daniel A. Oduma^a, Cecil N.M. Ouma^b, Eni Oko^c, Michael O. Daramola^a

^aSustainable Energy and Environment Research Group (SEERG), Department of Chemical Engineering, Faculty of Engineering, Built Environment and Information Technology, University of Pretoria, Hatfield 0028, Pretoria, South Africa

^bHySA Infrastructure Center of Competence, North-West University, Faculty of Engineering, P. Bag X6001, Potchefstroom 2520, South Africa

^cSchool of Engineering, Newcastle University, Newcastle upon Tyne NE1 7RU, UK

nomcebo.motsa@up.ac.za

Noble metals like Ruthenium (Ru) are widely used in various chemical reactions, especially for decomposing ammonia (NH₃). NH₃ is crucial for the hydrogen economy because it generates hydrogen, a versatile energy source and carrier. However, the high cost and scarcity of noble metals, including Ru, have limited large-scale deployment of NH₃ decomposition systems. This study investigates a solution known as noble metal thrifiting, which aims to address these challenges. Specifically, it examines the effectiveness of Ru supported on cerium oxide (CeO₂) in the form of single-atom catalysts (SACs) using density functional theory (DFT). The obtained results are compared with those of the pristine Ru(111) surface slab. The study observed that NH₃ binds more strongly to the Ru SAC system than its decomposition products, N₂ and H₂. Analysis of the activation energies shows that the dehydrogenation of NH₂ is the slowest step in NH₃ decomposition over CeO₂(111) and pristine Ru(111) catalysts with activation energies of 2.56 eV and 2.26 eV. The initial dehydrogenation of NH₃ is the slowest step in the Ru SAC catalyst, with an activation energy of 1.93 eV. The findings from this research are significant because they give credence to the potential of Ru thrifiting, particularly Ru SAC supported on CeO₂, as a probable means to utilize the efficacy of Ru in the decomposition of NH₃, without the limitations associated with noble metal scarcity and cost.

1. Introduction

The need to transition to clean and sustainable energy systems is imperative, given the adverse environmental effects associated with fossil fuel-based energy production (York and Bell., 2019) and rising climate change concerns (Rizeiqi et al., 2023). Numerous investigations have delved into sustainable energy alternatives, aiming to replace reliance on fossil fuels (Kapdan and Kargi, 2006). According to Guilbert and Vitale (2021), hydrogen is a promising energy carrier and is integral in the change to an environmentally friendly and sustainable source of energy. According to Hosseini and Wahid (2016), hydrogen is a clean fuel void of pollution, with an energy yield of about 122 kJ/g, which is 2.75 times greater than hydrocarbon fuels.

However, the main bottleneck to the deployment of hydrogen systems is its storage (Zheng et al., 2012). According to Aziz et al. (2020), although hydrogen can be liquefied and stored, a lot of energy goes into the liquefaction of hydrogen. Safety risks and high costs are known issues associated with liquid hydrogen storage (Mazloomi and Gomes, 2012). Ammonia (NH₃), however, has been identified by several researchers as a viable hydrogen storage option (Spatolisano et al., 2023). A major benefit of using NH₃ as feedstock for H₂ production is that large-scale production of NH₃ is well established (about 100 Mt/y of NH₃) (Langmi et al., 2022). It readily condenses under compression at 1 MPa and 298 K, and it boasts a substantial hydrogen content by weight, measuring 17.8 %, and achieves a volumetric hydrogen density surpassing liquid hydrogen by over 1.5 times (Kojima and Yamaguchi, 2020).

Ruthenium (Ru) catalyst is known to be the most efficient for ammonia decomposition (Su et al., 2023). It has been observed to possess superior catalytic activity in NH_3 decomposition at relatively low temperatures. Hence, it has been the subject of significant study in recent years (Casu, 2022). Even though Ru has good catalytic properties, it is not always the first choice due to several factors. Firstly, ruthenium is scarce and costly (Wenger, 2019), which poses a draw-back to its implementation. Secondly, the global supply of ruthenium is limited, which can lead to supply chain challenges and price volatility (Renner and Wellmer, 2020). Lastly, ruthenium compounds can be toxic, which might limit their use where safety is a concern (Mello-Andrade et al., 2018). Attempts have been made to look for Ru alternatives (Lu et al., 2021). It is speculated that a reduction in the amount of Ru required for the reaction might serve to make its utilization viable. This reduction can be achieved through single atom catalysts (SACs) i.e. Ru thrifiting. In Ru thrifiting, small amounts of Ru are utilized that achieve comparable yield/activity attained during utilization of pristine Ru catalyst, without a compromise in quality.

According to Yan et al. (2023), SACs have the potential to significantly reduce the required metal loading, reducing the cost of the catalyst. Additionally, according to Wu et al. (2023), SACs facilitate the characterization and identification of active sites, enhancing the understanding of the structure-property relationship at the atomic level in catalytic reactions. Use of SACs maximizes atom utilization and ensures high dispersion, which bolsters catalytic efficiency, activity and selectivity, with metal-support interactions contributing to the stability of SACs. Studies have shown SACs to possess superior catalytic properties in comparison to its pristine counterpart. For instance, Lang et al. (2020) reported that single-atom Ir/FeOx, Rh/TiO₂, and Pd/FeOx showed excellent catalytic activity in comparison to conventional catalyst in a Water Gas Shift Reaction, with Ir/FeOx exhibiting over 10 times more activity than the Ir nanoparticle (Ding et al., 2019). The success of SACs is enormous. Hence, its application in several processes has been widely studied.

To our knowledge, no study has been conducted into utilisation of Ru SAC in NH_3 decomposition. The novelty of this study is that it investigates Ru SACs feasibility in NH_3 decomposition. Contrary to the common practice of replacing Ru to reduce cost, this study advocates for a measured use of Ru in the appropriate quantities to yield the same performance while mitigating the cost constraint, paving the way for an economically feasible adoption of Ru catalyst for NH_3 decomposition. In this study, the Ru SAC will be supported on a cerium oxide (CeO_2) support. CeO_2 is chosen as the support for the Ru SAC due to its characteristic as a catalyst and a support. According to Lang et al. (2020) one highly appealing aspect of CeO_2 is its vacancy density, which facilitates the stabilization of individual metal atoms. Additionally, its tendency to stabilize transition metals in a dispersed state, positions CeO_2 as a potent support material in various catalytic conversions (Lang et al., 2020). Moraes et al. (2023) successfully utilised the CeO_2 support to improve the selective activation of methane for H_2 production. Against this background, this study aims to investigate if Ru SACs can produce the same performance as pristine Ru, or at least come close to that of pristine Ru for NH_3 decomposition.

2. Computational Details

All calculations were carried out using density functional theory (DFT) as implemented in the Dmol³ module (Delley, 2000) in Material Studio software (Biovia, 2017). The Perdew-Burke-Ernzerhof (PBE) gradient-corrected functional (Perdew, Burke and Ernzerhof, 1996) and the double numerical plus d-functions (DND) (Delley, 1990) are used to describe the exchange and correlation energy. DFT Semi-core Pseudopotential was selected for treatment of core electrons. Monkhorst–Pack grid (Monkhorst and Pack, 1976) was used to sample the Brillouin zone; a Monkhorst–Pack $2 \times 2 \times 1$ k-point grid was utilized for the pristine Ru(111), while k-point grid of $3 \times 3 \times 1$ was used for Ru SAC and the $\text{CeO}_2(111)$. Calculations were carried out using the spin-polarization method in order to account for magnetic properties, while a Fermi smearing of 0.05 Ha and a self-consistent field (SCF) tolerance of $1.0e^{-5}$ was utilized to improve computational performance. For geometry optimisations, the convergence threshold for the maximum energy change, maximum force, and maximum displacement were set as $2.0e^{-5}$ Ha, 0.004 Ha/Å, and 0.005 Å. In the transition state search a complete Linear Synchronous Transit and Quadratic Synchronous Transit (LST/QST) was utilized as the synchronous transit search protocol, and a Root Mean Square (RMS) convergence was set as 0.01 Ha/Å.

The SAC support, $\text{CeO}_2(111)$, was modelled as a 9 layer slab with a (1×1) unit cell, while the pristine Ru(111) catalyst was modelled as a 9 layer slab with a (2×2) unit cell. The bottom 4 layers of the respective structures were frozen but the remaining layers as well as the adsorbates were allowed to relax during geometry optimizations. A vacuum spacing of 15 Å was utilized to prevent interactions between repeating images in the z direction.

In the determination of the optimal surface on the $\text{CeO}_2(111)$ to be utilized for the Ru SAC, several surface terminations of the $\text{CeO}_2(111)$ as shown in Figure 1, were geometry optimized, then the surface with the minimum energy was identified as the optimal surface.

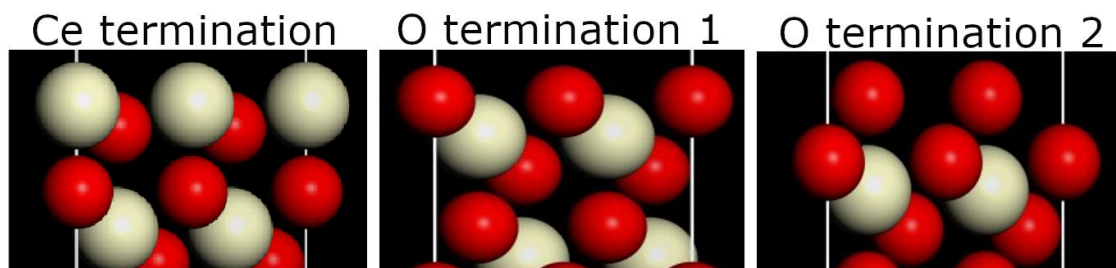


Figure 1: Surface terminations of $\text{CeO}_2(111)$; Red balls represent O atom while cream white balls represent Ce atom.

The adsorption energy of the Ru atom on the surface of the $\text{CeO}_2(111)$ at various sites was then calculated according to Equation 1, then the site with the minimal adsorption energy was determined to be the preferred adsorption site for Ru on the $\text{CeO}_2(111)$ surface. The preferred adsorption sites of the adsorbates on the Ru SAC, pristine Ru(111) and $\text{CeO}_2(111)$ were then determined similarly.

$$E_{\text{adsorption}} = E_{(\text{surface} + \text{Adsorbate})} - E_{(\text{Surface})} - E_{(\text{Adsorbate})} \quad (1)$$

Where $E_{\text{adsorption}}$ is adsorption energy, $E_{(\text{surface} + \text{Adsorbate})}$ is the energy of the surface and the adsorbate, $E_{(\text{Surface})}$ is the energy of the surface only, and $E_{(\text{Adsorbate})}$ is the energy of the adsorbate molecule.

For the transition state search, all the layers of the respective structures were frozen, while the adsorbates were allowed to relax. The activation energies (E_a) were then attained according to Equation 2:

$$E_a = E^{TS} - E^S \quad (2)$$

Where E_a is the activation energy, E^{TS} is the enthalpy of the transition state, and E^S is the enthalpy of the reactant.

The flow chart shown in Figure 2 provides a summary of the procedure utilised in this study.

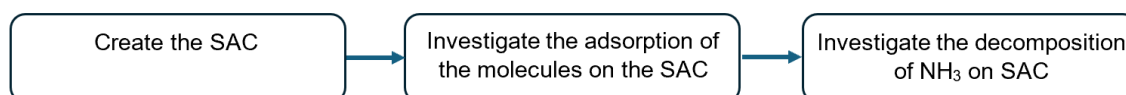


Figure 2: Process flow diagram

3. Results and Discussion

3.1 Adsorption of the Ru atom to the $\text{CeO}_2(111)$ surface

Several terminations of the $\text{CeO}_2(111)$ were investigated in order to attain the most stable surface terminations. The total energy obtained from the geometry optimization of the various surface terminations of the $\text{CeO}_2(111)$, as shown in Table 1, showed that the most stable termination is the O terminated surface, with an adsorption energy of -71198.89 eV.

Table 1: Energies of the various CeO_2 surface terminations

surface termination	Energy (eV)
O termination 1	-71198.89
Ce termination	-71189.97
O termination 2	-71189.39

Upon investigating the adsorption of Ru on atop, hcp, fcc and bridge sites on the $\text{CeO}_2(111)$ surface, it was observed that the preferred adsorption site of the Ru atom on the $\text{CeO}_2(111)$ support is in an fcc position, with an adsorption energy of 0.87 eV. Figure 3 depicts the optimal adsorption site of the Ru atom on the support.

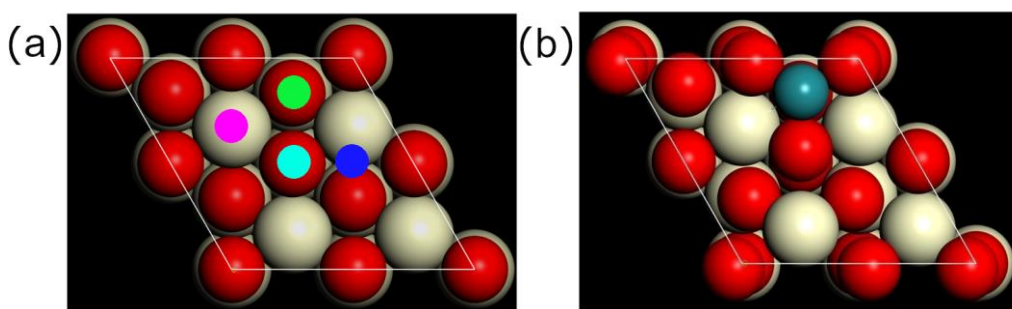


Figure 3: (a) The various sites investigated for Ru adsorption on CeO₂ surface. The sites depicted in lilac, green, turquoise, and blue refer to hcp, fcc, atop and bridge sites. (b) The stable adsorption site of Ru on the CeO₂(111) support; Teal blue, red, and cream white balls represent Ru, O and Ce atoms.

3.2 Adsorption of the different molecules on the catalysts surface

The preferred adsorption sites of the molecules involved in the decomposition of NH₃ was determined on the CeO₂(111), Ru(111) and the Ru SAC. These are portrayed in Figure 4.

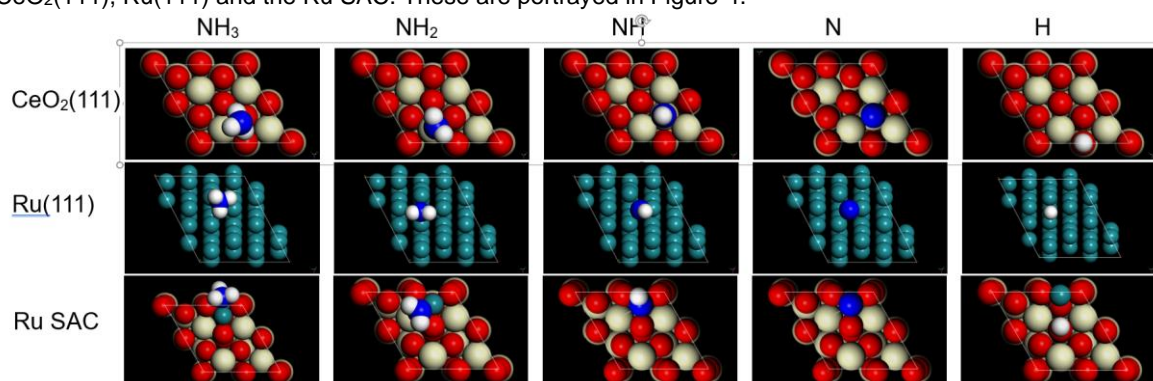


Figure 4: The stable adsorption site of the adsorbates on the CeO₂(111), Ru(111) and Ru SAC surfaces; Teal blue, white, red, cream white balls, and blue represent Ru, H, O, Ce, and N atoms.

Table 2: Adsorption energies of the adsorbates on the catalysts surface

Adsorbate	CeO ₂ (111) (eV)	Ru(111) (eV)	Ru (SAC) (eV)
H ₂	-0.18	-0.18	-0.26
N ₂	-0.73	-1.58	-1.22
H	-2.9	-2.49	-2.55
N	-4.72	-5.87	-4.65
NH	-3.03	-5.1	-4.09
NH ₂	-2.53	-3.45	-3.28
NH ₃	-1.45	-2.08	-1.72

The adsorption energies of the various molecules on these sites were determined and are listed in Table 2. It is observed that the adsorption energy of the various molecules on the Ru SAC surface is negative, which implies its feasibility. It is further observed that the adsorption energies of the adsorbates on the pristine Ru and the Ru SAC surfaces are very close, which implies that the adsorbate interacts similarly with the pristine Ru and the Ru SAC. In addition, the variation between the adsorption energies obtained from the CeO₂(111) surface and those from the Ru SAC, as shown in Table 2, shows that the presence of the Ru atom improves the adsorption of the adsorbates on the catalyst surface. From the adsorption energies of the adsorbates on the Ru SAC, it is observed that NH₃ binds more strongly than its decomposition products H₂ and N₂, which indicates that minimal energy will be required to desorb the reaction products from the face of the catalyst. Furthermore, it is observed

that N binds more strongly to the face of the respective catalysts than all other adsorbates, with adsorption energies of -4.72 eV, -5.87 eV, and -4.65 eV on the CeO₂(111), pristine Ru, and Ru SAC surfaces. These values indicate that lesser energy is required to desorb N from the surface of the Ru SAC catalyst than from the surface of the CeO₂(111) catalyst and the pristine Ru(111) catalyst. This suggests that utilization of the Ru SAC reduces the possibility of N atoms clogging up the active sites on the catalyst surface

3.3 Activation energies of the stepwise decomposition of NH₃ on the various catalyst

Lu et al. (2021) depicted that the activation energies for the dehydrogenation of NH₃, NH₂ and NH over a Ru(111) catalyst at 473 K are about 1.17 eV, 0.69 eV, and 1.73 eV. However, since it is imperative that decomposition of NH₃ over Ru is investigated at similar DFT conditions. NH₃ decomposition over pristine Ru(111) was also investigated in this study, and all attained activation energies in this study are shown in Table 3. Analysis of the activation energies attained shows that the activation energy obtained with the Ru SAC is mostly considerably lower than those attained over the pristine Ru(111) surface. This alludes to the efficacy of the Ru SAC in comparison to the pristine Ru(111) catalyst. It was observed that the slowest step in the decomposition of NH₃ over the CeO₂(111) surface and the Ru(111) surface is the NH₂ dehydrogenation step, with activation energies of 2.56 eV and 2.26 eV, while the slowest step pertaining to decomposition over Ru SAC surface is the NH₃ dehydrogenation step, with an activation energy of 1.93 eV. Based on these values it is speculated that since the maximum energy barrier in the reaction over the Ru SAC is lower than that from the pristine Ru(111), the reaction will proceed much faster over the Ru SAC surface in comparison to the pristine surface. This shows that utilization of the Ru SAC could potentially reduce the inherent cost of NH₃ decomposition

Table 3: Activation energies of the various reactions

Adsorbate	CeO ₂ (eV)	Ru(111) (eV)	Ru (SAC) (eV)
NH ₃ --> NH ₂ + H	2.12	2.02	1.93
NH ₂ --> NH + H	2.56	2.26	1.71
NH --> N + H	2.23	1.65	1.88
N + N --> N ₂	0.16	1.29	0.30
H + H --> H ₂	3.32	0.40	0.20

4. Conclusions

The catalytic decomposition of NH₃ over the surface of a pristine CeO₂(111), a pristine Ru(111), and a Ru SAC has been investigated. Based on the adsorption energies, it was found that the respective molecules (NH₃ and its decomposition by-products) interact with the surface of the Ru SAC in a similar manner to the pristine Ru(111) catalyst surface. Analysis of the activation energies suggests that NH₃ decomposition easily occurs over a Ru SAC in comparison to the pristine Ru catalyst; this is evident in the 4.31 % difference in the activation energies attained for NH₃ dehydrogenation over the respective catalysts. Additionally, the activation energy for H₂ formation over Ru SAC was observed to be 0.30 eV which is 49.32 % lower than the activation energy over the pristine Ru(111) catalyst. Similarly, a 76.84 % lower activation energy was also observed for N₂ formation. These results suggest that Ru SAC can probably be used in place of the pristine Ru slab. However, further investigation into the respective kinetics of the reactions is required for a more comprehensive investigation of the catalyst's efficacy.

Acknowledgments

The authors extend their profound gratitude to the Centre for High Performance Computing (CHPC), Cape Town, South Africa for the computational resources used in this study, and their profound assistance in all instances it was required. We further extend our gratitude to Proconics for their financial support.

References

- Aziz M., Wijayanta A.T., Nandiyanto A.B.D., 2020, Ammonia as effective hydrogen storage: A review on production, storage and utilization. *Energies*, 13(12), 3062.
- Biovia D.S., 2017, Materials studio. R2 Dassault Systèmes BIOVIA, San Diego, CA, USA.
- Casu S., 2022, Ruthenium-based catalysts and ammonia cracking. *The Catalyst Review*, 6, 6-11.

- Delley B., 1990, An all-electron numerical method for solving the local density functional for polyatomic molecules. *The Journal of Chemical Physics*, 92(1), 508-517.
- Delley B., 2000, From molecules to solids with the DMol3 approach. *The Journal of Chemical Physics*, 113(18), 7756-7764.
- Ding S., Hülsey M.J., Perez-Ramirez J., Yan N., 2019, Transforming energy with single-atom catalysts. *Joule*, 3(12), 2897-2929.
- Guilbert D., Vitale G., 2021, Hydrogen as a clean and sustainable energy vector for global transition from fossil-based to zero-carbon. *Clean Technologies*, 3(4), 881-909.
- Hosseini S.E., Wahid M.A., 2016, Hydrogen production from renewable and sustainable energy resources: Promising green energy carrier for clean development. *Renewable and Sustainable Energy Reviews*, 57, 850-866.
- Kapdan I.K., Kargi F., 2006, Bio-hydrogen production from waste materials, *Enzyme and Microbial Technology*, 38(5), 569-582.
- Kojima Y., Yamaguchi M., 2020, Ammonia storage materials for nitrogen recycling hydrogen and energy carriers. *International Journal of Hydrogen Energy*, 45(16), 10233-10246.
- Lang R., Du X., Huang Y., Jiang X., Zhang Q., Guo Y., Liu K., Qiao B., Wang A., Zhang T., 2020, Single-atom catalysts based on the metal–oxide interaction. *Chemical Reviews*, 120(21), 11986-12043.
- Langmi H.W., Engelbrecht N., Modisha P.M., Bessarabov D., 2022, Hydrogen storage in electrochemical power sources: Fundamentals, systems, and applications, Elsevier, Amsterdam, Netherlands, 455–486.
- Lu X., Zhang J., Chen W.K., Roldan A., 2021, Kinetic and mechanistic analysis of NH₃ decomposition on Ru (0001), Ru (111) and Ir (111) surfaces. *Nanoscale Advances*, 3(6), 1624-1632.
- Mazloomi K., Gomes C., 2012, Hydrogen as an energy carrier: Prospects and challenges. *Renewable and Sustainable Energy Reviews*, 16(5), 3024-3033.
- Mello-Andrade F., Cardoso C.G., e Silva C.R., Chen-Chen L., de Melo-Reis P.R., de Lima A.P., Oliveira R., Ferraz I.B.M., Grisolia C.K., Almeida M.A.P., Batista A.A., 2018, Acute toxic effects of ruthenium (II)/amino acid/diphosphine complexes on Swiss mice and zebrafish embryos. *Biomedicine & Pharmacotherapy*, 107, 1082-1092.
- Monkhorst, H.J., Pack, J.D., 1976. Special points for Brillouin-zone integrations. *Physical review B*, 13(12), 5188-5192.
- Moraes P.I.R., Bittencourt A.F., Andriani K.F., Da Silva J.L., 2023 Theoretical Insights into Methane Activation on Transition-Metal Single-Atom Catalysts Supported on the CeO₂ (111) Surface. *The Journal of Physical Chemistry C*, 127(33), 16357-16366.
- Perdew J.P., Burke K., Ernzerhof M., 1996, Generalized gradient approximation made simple. *Physical Review Letters*, 77(18), 3865.
- Renner S., Wellmer F.W., 2020, Volatility drivers on the metal market and exposure of producing countries. *Mineral Economics*, 33(3), 311-340.
- Rizeiqi N.A., Jedda M., Liew P.Y., 2023, Silica Sand as Thermal Energy Storage for Renewable-based Hydrogen and Ammonia Production Plants. *Chemical Engineering Transactions*, 106, 1111-1116.
- Spatolisano E., Pellegrini L.A., de Angelis A.R., Cattaneo S., Roccaro E., 2023, Ammonia as a carbon-free energy carrier: NH₃ cracking to H₂. *Industrial & Engineering Chemistry Research*, 62(28), 10813-10827.
- Su T., Guan B., Zhou J., Zheng C., Guo J., Chen J., Zhang Y., Yuan Y., Xie W., Zhou, N., Dang, H., 2023, Review on Ru-based and Ni-based catalysts for ammonia decomposition: research status, reaction mechanism, and perspectives. *Energy & Fuels*, 37(12), 8099-8127.
- Wenger O.S., 2019, Is iron the new ruthenium?. *Chemistry—A European Journal*, 25(24), 6043-6052.
- Wu J., Shi H., Li K., Guo X., 2023, Advances and challenges of single-atom catalysts in environmental catalysis. *Current Opinion in Chemical Engineering*, 40, 100923.
- Yan L., Li P., Zhu Q., Kumar A., Sun K., Tian S., Sun X., 2023, Atomically precise electrocatalysts for oxygen reduction reaction, *Chem*, 9(2), 280-342.
- York R., Bell S.E., 2019, Energy transitions or additions?: Why a transition from fossil fuels requires more than the growth of renewable energy. *Energy Research & Social Science*, 51, 40-43.
- Zheng J., Liu X., Xu P., Liu P., Zhao Y., Yang J., 2012, Development of high-pressure gaseous hydrogen storage technologies. *International Journal of Hydrogen Energy*, 37(1), 1048-1057.